AFRL-VS-TR-2003-1592

VALIDATION OF IONOSPHERIC MODELS

Patricia Doherty

Boston College
Institute for Scientific Research
140 Commonwealth Avenue
Chestnut Hill, MA 02467-3862

31 March 2001

Scientific Report No. 5

AIR FORCE RESEARCH LABORATORY
Space Vehicles Directorate
29 Randolph Rd
AIR FORCE MATERIEL COMMAND
Hanscom AFB, MA 01731-3010

"This technical report has been reviewed and is approved for publication"

/signed/

JOHN RETTERER
Contract Manager

/signed/

ROBERT MORRIS
Branch Chief

This report has been reviewed by the ESC Public Affairs Office (PA) and is releasable to the National Technical Information Service (NTIS).

Qualified requestors may obtain additional copies from the Defense Technical Information Center (DTIC). All others should apply to the National Technical Information Service (NTIS).

If your address has changed, if you wish to be removed from the mailing list, or if the addressee is no longer employed by your organization, please notify AFRL/VSIM, 29 Randolph Road, Hanscom AFB MA 01731-3010. This will assist us in maintaining a current mailing list.

Do not return copies of this report unless contractual obligations or notices on a specific document require that it be returned.

REPORT DOCUMENTATION PAGE

Form Approved
OMB No. 0704-0188

1. REPORT DATE *(DD-MM-YYYY)*	2. REPORT TYPE	3. DATES COVERED *(From - To)*
31-03-2001	Scientific Report No. 5	April 2000 - March 2001

4. TITLE AND SUBTITLE

VALIDATION OF IONOSPHERIC MODELS

5a. CONTRACT NUMBER
F19628-96-C-0039

5b. GRANT NUMBER

5c. PROGRAM ELEMENT NUMBER
61102F

6. AUTHOR(S)

Patricia H. Doherty

5d. PROJECT NUMBER
1010

5e. TASK NUMBER
IM

5f. WORK UNIT NUMBER
AC

7. PERFORMING ORGANIZATION NAME(S) AND ADDRESS(ES)

Boston College / Institute for Scientific Research
140 Commonwealth Avenue
Chestnut Hill, MA 02467-3862

8. PERFORMING ORGANIZATION REPORT NUMBER

9. SPONSORING/MONITORING AGENCY NAME(S) AND ADDRESS(ES)

Air Force Research Laboratory/VSBP
29 Randolph Road
Hanscom AFB, MA 01731-3010

10. SPONSOR/MONITOR'S ACRONYM(S)

11. SPONSOR/MONITOR'S REPORT NUMBER(S)
AFRL-VS-TR-2003-1592

12. DISTRIBUTION/AVAILABILITY STATEMENT

13. SUPPLEMENTARY NOTES

Approved for public release; distribution unlimited.

14. ABSTRACT

During the period of April 2000 through March 2001, research efforts have continued in the Validation of Ionospheric Models. These efforts included testing and utilizing the Ionospheric Forecast Model (IFM) and the Coupled Ionosphere Thermosphere Electrodynamic Forecast Model (CITEFM) to define low latitude ionospheric characteristics. Other efforts included continued validations of the Parameterized Real-time Ionospheric Specification Model (PRISM) and development of a data preprocessor that will allow various data types to be integrated into PRISM. Data analysis studies included the mid-latitude response to major magnetic storm activity. Work was also made to refine and transition the Global Positioning System (GPS) Single-Frequency Position Error Maps to the 55th Space Weather Squadron. This resulted in being part of the team that was awarded the Annual Air Force Merewether Award of 2000 for the Most Significant Technical Contribution. Finally, we contributed to the development of an alternate derivation of the Alfven-Falthammer formula for the parallel E-field in upward auroral-current regions.

15. SUBJECT TERMS

Ionosphere, IFM, CITEFM, PRISM, GPS, Total Electron Content (TEC), Position errors, OPerational Space Environment Network Display (OP-SEND)

16. SECURITY CLASSIFICATION OF:			17. LIMITATION OF ABSTRACT	18. NUMBER OF PAGES	19a. NAME OF RESPONSIBLE PERSON
a. REPORT	b. ABSTRACT	c. THIS PAGE			John Retterer
U	U	U	SAR		19b. TELEPHONE NUMBER *(Include area code)* 781-377-3891

TABLE OF CONTENTS

1. GOALS

The objective of this contract is to obtain ionospheric measurements from a wide range of geographic locations and to utilize the resulting databases to validate the theoretical ionospheric models that are the basis of the Parameterized Ionospheric Specification Model (PRISM) and the Ionospheric Forecast Model (IFM).

In the past year, we have supported these goals with the following activities:

- tested the IFM model.
- initiated the use and production of the Coupled Ionosphere Thermosphere Electrodynamic Forecast Model (CITEFM).
- developed an alternate derivation of the Alfven-Falthammer formula for the parallel *E*-field in upward auroral-current regions.
- contributed to validation studies of PRISM.
- analyzed the ionospheric response to the Great Magnetic Storm of July 2000.
- initiated validations of the Global Positioning System (GPS) position error maps.
- initiated development of a PRISM pre-processor that will enable data from various sensors to be integrated into the existing technology of PRISM.

These activities resulted in three presentations at various ionospheric meetings and one published journal article. Details of these activities, presentations and the journal article are provided in this report.

2. PROGRESS

2.1 The Ionospheric Forecast Model (IFM)

The IFM model is a collection of programs that provide a first-principles, global representation of the ionosphere given a set of geophysical conditions. In the current year, the IFM model was utilized to generate ionospheric characteristics for three levels of magnetic activity and three levels of solar activity. The Total Electron Content (TEC) and maximum density of the F2 region (NmF2) output from the nine IFM runs were graphically animated and displayed on a web site maintained by Boston College. Producing these animations facilitated AFRL's ability to identify the weaknesses of the model. This work resulted in several modifications to the IFM model.

2.2 The Coupled Ionosphere Thermosphere Electrodynamic Forecast Model (CITEFM)

In the current year, work was initiated to incorporate the CITEFM into applications at AFRL. The CITEFM model is a first-principles model that combines ionospheric, thermospheric and dynamo calculations to produce global simulations given a set of geophysical conditions. In the current year, we installed and utilized the CITEFM model to generate calculations of TEC, NmF2, density profiles and meridional and zonal winds. These calculations were produced for a

variety of geophysical conditions. Specialized software was developed to graphically analyze and animate the CITEFM output. This work was useful in detecting anomalous behavior in the model. As a result of these efforts, the model was revised to produce a more accurate representation of ionospheric parameters.

The work done this year using the IFM and CITEFM was useful in the initial plans of the Communications /Navigation Outage Forecast System (C/NOFS) science plan. The models were used to define and display the current level of knowledge that is built into the specification models used at AFRL. C/NOFS is a science plan to forecast the presence of equatorial ionospheric irregularities that may adversely affect communication and navigation satellite-based systems. It is comprised of a satellite that will be equipped with a variety of sensors to measure electron densities; ion and electron temperatures; magnetic fields, neutral winds, ionospheric scintillations; and TEC along the lines of sight between the C/NOFS and GPS satellites. The C/NOFS satellite will be launched in early 2004.

2.3 The Alfven-Falthammar Formula for the Parallel E-Field and Its Analogue in Downward Auroral-Current Regions

In the current year, efforts were expanded to explain the Birkeland current system. The Birkeland currents are a system of upward and downward magnetic field-aligned electrical currents in the auroral zone that flow between the magnetosphere and the ionosphere where particle number flux, momentum and energy flux are exchanged. The analysis used led to a set of differential equations. Several different sets of differential equations were analyzed. Each set of equations was analyzed in two steps. The first step involved using symbolic manipulation to triangularize the set of equations to solve. The final step of the analysis is a Fortran code, which solves the set of differential equations with given boundaries.

These formulas give new insight into the physics of the Birkeland current system. It was found that for downward auroral-current regions, the velocity-space anisotropy in the ion distribution function is such that half the ion energy perpendicular to the magnetic field is greater than the ion energy parallel to the magnetic field. This is just opposite to the case for upward auroral-current regions.

Details of this work together with the results were published in the IEEE Transactions on Plasma Science. A reprint of this article is attached to this annual report (see Appendix).

2.4 PRISM Validations

PRISM is a model developed by AFRL that specifies electron density of the ionosphere on a global and/or regional scale. PRISM is capable of ingesting data from three types of sensors: (1) ionospheric sounders; (2) TEC sensors; (3) in situ sensors on board Defense Meteorological Satellite Program (DMSP). PRISM then adjusts its climatological map to agree with the data taken at the various geographic locations.

In the current year, we have participated in continued efforts to determine the accuracy of PRISM calculations. The current efforts included defining the accuracy dependence with respect

to the number of stations used to drive the model. This effort required collecting and analyzing data from approximately 90 different geographic locations. Our efforts were primarily devoted to the analysis of the GPS TEC used in this work. The data was used to define how well the model calculations improve with increased data.

This work was presented at the AIAA Space 2000 Conference, Long Beach CA, September 2000.

2.5 The Great Magnetic Storm of July 2000

On July 14th, a coronal mass ejection left the Sun at a speed of 1800 km/s. Its effects on Earth were noted on July 15th in the form of an extreme geomagnetic storm with Kp values of 9 recorded from approximately 15 through 21 UT. A storm of this size can have a significant effect on TEC and consequently on sophisticated space-based technology systems, such as communication and navigation. In response to this storm, we obtained and analyzed worldwide GPS TEC data to determine the ionospheric behavior during this great storm. The most significant findings were the unprecedented magnitudes and gradients measured in TEC in the southeast region of the United States.

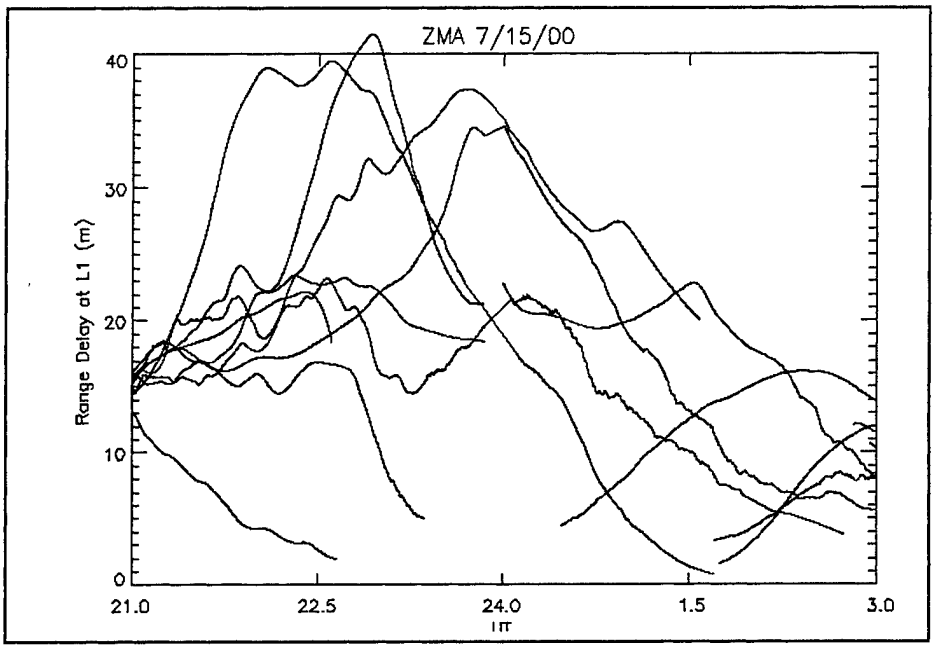

Figure 1. Equivalent Vertical Range Delay Measured from Miami During the Great Magnetic Storm of July 2000.

This is illustrated in Figure 1, where GPS measurements of equivalent vertical range delay recorded along multiple lines of sight from Miami, FL are plotted versus Universal Time (UT). Note that the range delays exceed 40 meters (equivalent to 240 TEC units) near 23UT. Also note the large spatial gradients observed along different lines of sight from the Miami receiver. All of these effects were unprecedented features of this mid-latitude location. This work together

additional storm analysis efforts was useful in defining mid-latitude response to severe geomagnetic storm activity.

2.6 GPS Position Error Maps

In the last two years, we worked to develop software to investigate navigational position errors caused by inaccuracies in the standard Ionospheric Corrections Algorithm (ICA). The work resulted in a model that estimates position errors for the single frequency user and displays these potential errors on a worldwide graphics display. Near the end of the last year, we also worked to incorporate this software into the Operational Space Environment Network Display (OP-SEND). The OP-SEND project is a graphic-based space environment forecasting tool that was made operational at the 55th Space Weather Squadron (SWXS). As a result of our efforts in the design of OP-SEND together with our participation in the transition of the OP-SEND product to SWXS, we were included in the team that was awarded the Annual Air Force Merewether Award for the year 2000. This award was in the category of Most Significant Technical Contribution.

OP-SEND includes maps with near real-time estimates on:

- UHF SATCOM Scintillation.
- HF Illumination.
- Auroral Clutter Boundaries.
- Scintillation Predictions.
- GPS Single-Frequency Position Errors.

In the current year, we have also continued to augment and support the GPS Single-Frequency Position Errors component of OP-SEND by designing a comprehensive validation effort to be conducted over the next two years of this contract.

This work resulted in a presentation at the American Geophysical Union meeting held in San Francisco, CA in December 2000.

2.7 Ultra-Violet (UV) PRISM

In the current year, work was initiated to develop a software product that will be used to integrate data from various sensors into the existing technology of the PRISM model.

Two UV sensors are planned to fly on the DMSP Block 5D-3 satellites. Both are remote-sensing instruments that measure ultraviolet emissions emitted by the Earth's upper atmosphere. One instrument is the Special Sensor Ultraviolet Limb Imager (SSULI), which scans the limb of the Earth in the orbital plane. It measures the UV emissions in the interval from 800 to 1700 Å. The other instrument is the Special Sensor Ultraviolet Spectrographic Imager (SSUSI), that measures emissions in five different wavelength bands. The resultant images cover the visible Earth disk from horizon to horizon and the anti-sunward limb up to an altitude of approximately 520 km.

These sensors have the potential to significantly improve ionospheric remote sensing. To take advantage of this opportunity, the data from these new sensors must be able to be used by operational products. Modifying PRISM to accept new data types is a difficult and time-consuming task. Therefore, we have initiated development of software that will accept the DMSP UV sensor data, extract the relevant data and convert it to a data type currently accepted by PRISM. This software will be called UV PRISM. Our initial work indicated that the data array sizes of PRISM were too small. This resulted in a modified PRISM model.

In the current year, we also simulated the UV measurements by using an authentic DMSP track, the International Reference Ionosphere Model (IRI) and the Parameterized Ionosphere Model (PIM). We utilized the simulated measurements as input to PRISM and to develop graphics that plot the results. These efforts allowed us to further understand the effect that the UV measurements will have on PRISM and to determine how to best utilize this new source of information.

This work is expected to fully develop in the next two years of this contract.

3. PRESENTATIONS

The work described in this report resulted in three oral presentations at various scientific meetings:

Bishop, G., Quigley, S., Groves, K., Bullett, T., Doherty, P., Cook, C., Citrone, P., Scro, K. and Wilkes, R., "OpSend: Mission-Tailored Graphical Products for DoD Warfighters," presented at the AGU Fall Meeting, San Francisco CA, December 2000.

Pulliam, R., Borer, W.S., Decker, D.T., and Doherty, P.H., "Operational Ionosphere Model Validations Study," presented at the AIAA Space 2000 Conference, Long Beach CA, September 2000.

Pulliam, R., Borer, W.S., Decker, D.T., and Doherty, P.H., "Evaluation of Metrics for Ambient Ionospheric Specification," presented at the AGU Fall Meeting, San Francisco CA, December 2000.

4. JOURNAL ARTICLES

Jasperse, J.R. and Grossbard, N.J., "The Alfven-Falthammer Formula for the Parallel *E*-Field and its Analogue in Downward Auroral-Current Regions," *IEEE Transactions on Plasma Science*, ***Vol. 28***, No. 6, December 2000.

5. AWARDS

Patricia H. Doherty and Susan H. Delay were part of the team that was awarded The Annual Air Force Merewether Award for the Year 2000 in the category of Most Significant Technical Contribution.

APPENDIX

The Alfvén–Fälthammar Formula for the Parallel E-Field and its Analogue in Downward Auroral-Current Regions

John R. Jasperse and Neil J. Grossbard, *Member, IEEE*

***Abstract*—In this paper, we give an alternative derivation of the Alfvén–Fälthammar formula for a positive parallel E-field in upward auroral-current regions and its analogue for a negative parallel E-field in downward auroral-current regions. These formulas give new insight into the physics of the Birkeland current system. We find that for downward auroral-current regions, the velocity-space anisotropy in the ion distribution function is such that half the ion energy perpendicular to the magnetic field is greater than the ion energy parallel to the magnetic field. This is just opposite to the case for upward auroral-current regions. These results are compared to recent particle-in-cell simulations and FREJA satellite data.**

***Index Terms*—Alfvén–Fälthammar formula, Birkeland current system, parallel E-fields in space plasmas.**

I. Introduction

THIS paper deals with the theory of the Birkeland current system which was discovered nearly 100 years ago and remains an active area of space physics research to this day. The Birkeland currents are a system of upward and downward magnetic field-aligned electrical currents in the auroral zone that flow between the magnetosphere and the ionosphere where particle number flux, momentum, and energy flux are exchanged. In our view, there is no problem more important to the understanding of space weather at high latitudes than to understand how the Birkeland current system works. For a study of the statistical properties of the Birkeland currents using TRIAD satellite data, see [1, Fig. 13]. For a recent case study using FAST satellite data, see [2, Fig. 3].

One of the purposes of this paper is to give an alternative derivation of the Alfvén–Fälthammar (A–F) formula for the parallel E-field ($E_{\|}$) in upward auroral-current regions. There are several ways to derive this result [3]–[6]. The formulas for $E_{\|}$ are the same but the derivations are not equivalent since different assumptions, closure approximations, and boundary conditions are used. Our derivation begins with the Vlasov equations and, as we will show, not only gives new insight into the physics of that problem, but may be generalized in a straightforward way to study downward auroral-current regions.

Manuscript received January 20, 2000; revised March 21, 2000.

J. R. Jasperse is with the Air Force Research Laboratory, Space Vehicles Directorate, Hanscom AFB, MA 01731 USA.

N. J. Grossbard is with Boston College, Institute for Scientific Research, Chestnut Hill, MA 02467 USA.

Publisher Item Identifier S 0093-3813(00)11345-1.

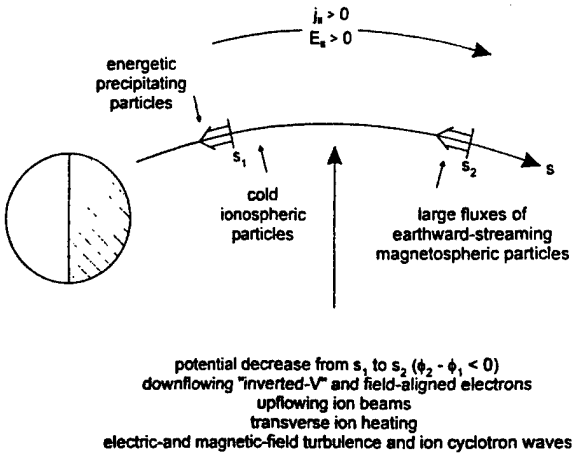

Fig. 1. Some properties of upward auroral-current regions.

The primary purpose of this paper, therefore, is to give the analogue of the A–F formula for $E_{\|}$ for downward auroral-current regions. The derivation begins with a velocity-space diffusion model for the problem, and the formula that we give for $E_{\|}$ also gives new insight into the physics of that problem.

There is a vast literature on upward auroral-current regions. For a review of rocket and satellite measurements before 1980, see [7]. For a sample of more recent satellite measurements, see [8] on FREJA results and FAST results in [9]. For example, the properties of upward auroral-current regions have been observed by the ISIS-1 [10], S3-3 [7], NOAA-6 [11], DE-1 [12], DE-2 [13], FREJA [14], POLAR [15], and FAST [16] satellites, to name a few. From these studies, we see that upward auroral-current regions are often characterized by

1) converging electrostatic shocks, upward pointing $E_{\|}$;
2) downflowing "inverted-V" and field-aligned electrons;
3) large-scale density cavities;
4) upflowing ion beams and transverse ion heating;
5) electric- and magnetic-field turbulence and ion cyclotron waves;
6) large fluxes of earthward-streaming energetic (> few kilovolts) magnetospheric particles.

Some of these properties are illustrated in Fig. 1 (not to scale). The theoretical literature before 1993 is reviewed in [17]. For a more recent review, see [18, Introduction and Bibliography].

The properties of downward auroral-current regions are less-explored. They have been observed by the ISIS-2 [19], DE-1

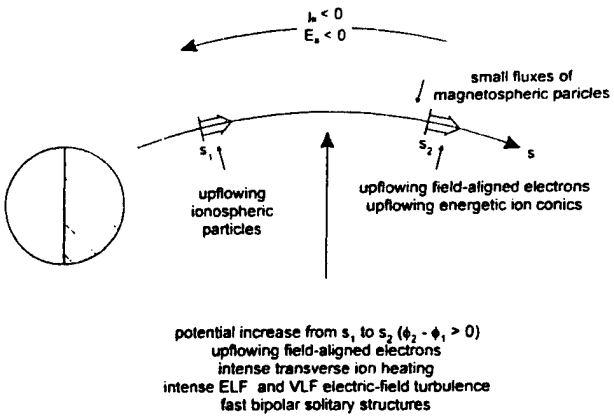

Fig. 2. Some properties of downward auroral-current regions.

[20], S3-3 [21], FREJA [22], FAST [23], [24], and other satellites. These downward currents often occur in the auroral zone adjacent to "inverted-V" structures [2], the dayside cusp-cleft region [21], and in association with the "black aurora" [25]. From these studies, we see that downward auroral-current regions are often characterized by

1) diverging electrostatic shocks, downward pointing $E_\parallel$;
2) upflowing low energy (< few kilovolts) field-aligned electrons;
3) intense transverse ion heating;
4) small-scale density cavities;
5) intense ELF and VLF electric-field turbulence and fast bipolar solitary structures;
6) small fluxes of energetic (> few kilovolts) magnetospheric particles.

Some of these properties are illustrated in Fig. 2 (not to scale). Some theoretical work has been carried out for downward auroral-current regions using the multimoment fluid equations for the current-driven ion cyclotron instability [26]; particle-in-cell (PIC) simulations in the electrostatic approximation [27], [28]; and a velocity-space diffusion model for the problem [29], [30].

In Section II, we give the alternative derivation of the A–F formula for a positive $E_\parallel$ in an upward auroral-current region, and, in Section III, its analogue for a negative $E_\parallel$ in a downward auroral-current region. In Section IV, we discuss these results.

II. Parallel E-Field Due to Injected Magnetospheric Particles in Upward Auroral-Current Regions

The purpose of this Section is to give an alternative derivation of the Alfvén–Fälthammar (A–F) formula for the parallel E-field ($E_\parallel$) in upward auroral-current regions. The original derivation is given in [3]. Although we obtain the same formula for $E_\parallel$, the method we use is different. Our reason for presenting an alternative derivation here is that the method we use may be easily generalized and applied to downward auroral-current regions, as we will see in Section III.

A. Vlasov Equations and the Quasi-Neutrality Condition

Upward auroral-current regions are often characterized by earthward-streaming energetic magnetospheric particles, the presence of low-energy (or ambient) ionospheric particles, and wave-particle interactions. The simplest way to model an auroral arc that we can think of is to neglect the ambient ionospheric particles and wave-particle interactions, and to consider only the injected magnetospheric particles. In his review, Borovsky [17] discusses 12 mechanisms by which the auroral plasma can sustain an $E_\parallel$, thereby accelerating auroral particles, and also ten drivers (or generators) of the mechanisms. As we will see in this section, the A–F formula for a positive $E_\parallel$ in upward auroral-current regions results from the following simple model for a quasi-stable auroral arc 1) the driver is the earthward-streaming energetic magnetospheric particles and 2) the mechanism that sustains $E_\parallel$ is the differential velocity-space anisotropy between the ions and the electrons in the dipolar magnetic field.

In this paper, we assume that the gyrotropic approximation is valid and seek a steady-state solution. The Vlasov equations in one-spatial and two-velocity dimensions are

$$\left\{ v_\parallel \frac{\partial}{\partial s} + \left[g_\parallel + \frac{q_\alpha}{m_\alpha} E_\parallel \right] \frac{\partial}{\partial v_\parallel} - \frac{1}{2B} \frac{dB}{ds} \left[v_\perp^2 \frac{\partial}{\partial v_\parallel} - v_\parallel v_\perp \frac{\partial}{\partial v_\perp} \right] \right\} f_\alpha = 0 \quad (1)$$

and the quasi-neutrality (Q-N) condition is

$$n_e = \sum_\beta n_\beta \quad (2)$$

where β is summed over the ions. Here, $g_\parallel$ and $E_\parallel$ are the parallel components of the gravitational acceleration and the electrostatic field, respectively; B is the geomagnetic field; $f_\alpha = f_\alpha(s, v_\perp, v_\parallel)$ is the gyrotropically-averaged distribution function for each species α; and s is the distance from the earth along the geomagnetic flux tube. Also, f_α is normalized to the particle density, n_α, and the other quantities have their usual meanings.

In (2), we have replaced Poisson's equation with the Q-N condition. This greatly simplifies the problem. The standard argument for making this replacement is that for length scales which are long compared to the Debye length, the two are equivalent. However, this is not at all obvious since, in making this replacement, we have completely changed the nonlinear character and boundary conditions of the problem. Much has been written about this issue [4]–[6], [31]–[33].

B. A–F Solution for $E_\parallel$ and Related Quantities from the Multimoment Fluid Equations

We now proceed to derive the multimoment fluid equations by multiplying (1) by $v_\perp^n v_\parallel^\ell$ and integrating over all velocity space. We use the following notation:

$$\langle v_\perp^n, v_\parallel^\ell \rangle_\alpha = \langle n, \ell \rangle_\alpha = 2\pi \int_{-\infty}^{\infty} dv_\parallel \int_0^\infty dv_\perp v_\perp^{1+n} v_\parallel^\ell f_\alpha(s, v_\perp, v_\parallel) \quad (3)$$

$$\dot{A} = -B^{-1}\, dB/ds = A^{-1}\, dA/ds \quad (4)$$

where A is the cross sectional area of the flux tube. Here n and ℓ are positive integers or zero. We obtain for all n and $\ell = 0$

$$d/ds\langle n, 1 \rangle_\alpha + \dot{A}(1 + n/2)\langle n, 1 \rangle_\alpha = 0 \quad (5)$$

and for all n and $\ell \geq 1$

$$d/ds\langle n, \ell+1\rangle_\alpha + \dot{A}(1+n/2)\langle n, \ell+1\rangle_\alpha + \ell\{(q_\alpha/m_\alpha)(d/ds\Phi_{\alpha\|})\langle n, \ell-1\rangle_\alpha - (\dot{A}/2)\langle n+2, \ell-1\rangle_\alpha\} = 0. \quad (6)$$

Here, $\Phi_{\alpha\|} = \phi_\| + (m_\alpha/q_\alpha)\phi_{G\|}$, where $\phi_\|$ is the electrostatic potential and $\phi_{G\|}$ is the gravitational potential. The multimoment fluid equations for $n = 0$, $\ell = 0$; $n = 0$, $\ell = 1$; $n = 0$, $\ell = 2$; and $n = 2$, $\ell = 0$ are

$$d/ds\, n_\alpha u_\alpha + \dot{A} n_\alpha u_\alpha = 0 \quad (7)$$

$$d/ds\, n_\alpha w_{\alpha\|} + \dot{A} n_\alpha (w_{\alpha\|} - w_{\alpha\perp}/2) + (q_\alpha/2) n_\alpha\, d/ds\Phi_{\alpha\|} = 0 \quad (8)$$

$$d/ds\, n_\alpha Q_{\alpha\|} + \dot{A} n_\alpha (Q_{\alpha\|} - Q_{\alpha\perp}) + q_\alpha n_\alpha u_\alpha\, d/ds\Phi_{\alpha\|} = 0 \quad (9)$$

$$d/ds\, n_\alpha Q_{\alpha\perp} + 2\dot{A} n_\alpha Q_{\alpha\perp} = 0. \quad (10)$$

Here, we have introduced the standard definitions $\langle 0,0\rangle_\alpha = n_\alpha$; $\langle 0,1\rangle_\alpha = n_\alpha u_\alpha$; $m_\alpha\langle 2,0\rangle_\alpha/2 = n_\alpha w_{\alpha\perp}$; $m_\alpha\langle 0,2\rangle_\alpha/2 = n_\alpha w_{\alpha\|}$; $m_\alpha\langle 2,1\rangle_\alpha/2 = n_{\alpha\perp} Q_{\alpha\perp}$; and $m_\alpha\langle 0,3\rangle_\alpha/2 = n_\alpha Q_{\alpha\|}$. The Qs denote the energy flux and should not be confused with the heat flux. Also, by definition, $w_{\alpha\perp} = T_{\alpha\perp}$ and

$$w_{\alpha\|} = T_{\alpha\|}/2 + m_\alpha u_\alpha^2/2$$

where the temperatures are expressed in energy units. Adding (9) and (10) together and using (7), we may obtain an alternative equation for (9). Equations (7)–(10) may then be rewritten as

$$B\, d/ds(n_\alpha u_\alpha/B) = 0 \quad (11)$$

$$d/ds(n_\alpha w_{\alpha\|}) - B^{-1}\, dB/ds\, n_\alpha(w_{\alpha\|} - w_{\alpha\perp}/2) + n_\alpha(q_\alpha/2)\, d/ds\, \Phi_{\alpha\|} = 0 \quad (12)$$

$$B\, d/ds\{[n_\alpha Q_{\alpha\|} + n_\alpha Q_{\alpha\perp} + q_\alpha n_\alpha u_\alpha \Phi_{\alpha\|}]/B\} = 0 \quad (13)$$

$$B^2\, d/ds(n_\alpha Q_{\alpha\perp}/B^2) = 0. \quad (14)$$

Equations (11)–(14) are the standard conservation laws for the number flux, momentum, total energy flux, and perpendicular energy flux, respectively.

Formal expressions for $E_\|$ may be found from (12) and (13) by simply rearranging the terms. Neglecting gravity, we see from momentum conservation (12) that

$$E_\| = (2/q_\alpha)\{-B^{-1}\, dB/ds(w_{\alpha\|} - w_{\alpha\perp}/2) + n_\alpha^{-1}\, d/ds\, n_\alpha w_{\alpha\|}\} \quad (15)$$

and from total energy flux conservation (13) with the help of (11) that

$$E_\| = (B/q_\alpha n_\alpha u_\alpha)\, d/ds[(n_\alpha Q_{\alpha\|} + n_\alpha Q_{\alpha\perp})/B]. \quad (16)$$

Equations (15) and (16) are 2α expressions for $E_\|$ in terms of the moments of f_α. We call them self-consistent formulas for $E_\|$ since, once the explicit solution for the moments of f_α are found, then (15) and (16) must be satisfied.

Equations (11)–(14) and (2) are $4\alpha + 1$ equations for $6\alpha + 1$ unknowns including the electrostatic potential $\phi_\|$. In order to solve them, we must introduce closure approximations. The standard procedure for closing the multimoment fluid equations is to use the gyrotropic limit of the Maxwellian-based 5-, 8-, 10-, or 13-moment sets, or the bi-Maxwellian-based 6- or 16-moment sets. For a discussion of this procedure, see [34]. Specific solutions have also been worked out for a variety of plasma-flow conditions [35], [36]. Instead of using the standard procedure, we use a simpler closure approximation which, as we shall see later in this section, places a restriction on the type of flow conditions to which it may be applied. The closure we use is

$$Q_{\alpha\perp} \cong u_\alpha w_{\alpha\perp} \quad (17)$$

$$Q_{\alpha\|} \cong u_\alpha w_{\alpha\|}. \quad (18)$$

Using (11), (17), and (18), we find that the multimoment fluid equations become

$$d/ds(n_\alpha u_\alpha/B) = 0 \quad (19)$$

$$d/ds\, n_\alpha w_{\alpha\|} - B^{-1}\, dB/ds\, n_\alpha(w_{\alpha\|} - w_{\alpha\perp}/2) + n_\alpha(q_\alpha/2)\, d/ds\, \Phi_{\alpha\|} = 0 \quad (20)$$

$$d/ds(w_{\alpha\|} + w_{\alpha\perp} + q_\alpha\Phi_{\alpha\|}) = 0 \quad (21)$$

$$d/ds(w_{\alpha\perp}/B) = 0 \quad (22)$$

$$n_e = \sum_\beta n_\beta, \qquad \beta = \text{ions}. \quad (23)$$

A few remarks about (19)–(23) are in order here. First, they are a set of $4\alpha + 1$ nonlinear, first-order ordinary differential equations for $4\alpha + 1$ unknowns subject to boundary conditions imposed at either end of the flux tube. Second, the closure approximation that we have used has, in effect, replaced the conservation of total energy flux (13) and the conservation of perpendicular energy flux (14), both of which are rigorous, by conservation relations for the total energy (21) and the perpendicular energy (22). These are just the conservation relations that we obtain from single-particle orbit theory. However, the concept of parallel and perpendicular temperature has been preserved in (19)–(23) as $w_{\alpha\perp} = T_{\alpha\perp}$ and $w_{\alpha\|} = T_{\alpha\|}/2 + m_\alpha u_\alpha^2/2$. Third, when anomalous transport effects are neglected, (19) and (20) are identical to the steady-state versions of (1) and (2) in [37], where the authors have used the gyrotropic limit of the 16-moment set to study the polar wind. However, (21) and (22) differ from the higher order moment equations in [37], as the closure approximation is different.

Now, we proceed to solve (19)–(23) in closed form subject to appropriate boundary conditions. Consider $s_1 \leq s \leq s_2$, where s_1 is in the ionosphere and s_2 is in the magnetosphere. Equation (20) may be further simplified. We may eliminate $\Phi_{\alpha\|}$ from (8) and (9) and use closure to obtain

$$d/ds\, n_\alpha u_\alpha w_{\alpha\|} - 2u_\alpha\, d/ds\, n_\alpha w_{\alpha\|} - \dot{A} n_\alpha u_\alpha w_{\alpha\|} = 0.$$

Using (7), we may further simplify to obtain

$$2w_{\alpha\|}\, dn_\alpha/ds + 2\dot{A} n_\alpha w_{\alpha\|} + n_\alpha\, dw_{\alpha\|}/ds = 0.$$

The left-hand side of this expression is proportional to $d/ds(n_\alpha^2 w_{\alpha\|}/B^2)$ which is in turn proportional to $d/ds(w_{\alpha\|}/u_\alpha^2)$, so (20) may be replaced by

$$d/ds(w_{\alpha\|}/u_\alpha^2) = 0. \quad (24)$$

The hidden meaning of the closure approximation given by (18) is now revealed. If the ratio $(T_{\alpha\|}/2 + m_\alpha u_\alpha^2/2)/(m_\alpha u_\alpha^2/2)$ does not change by very much on the flux tube, then (18) is a reasonable approximation. This requires that $T_{\alpha\|}$ and $m_\alpha u_\alpha^2$

change proportionally from s_1 to s_2 so that the above ratio is nearly constant. If we examine the experimental data and find that this approximation is valid, then (18) is a good closure approximation. However, we note that this closure may not apply to problems where the plasma flow evolves from subsonic to supersonic. We now integrate (22), (21), (24), and (19) from s to s_2, in that order, to find $w_{\alpha\perp}$, $w_{\alpha\parallel}$, u_α and n_α in terms of $\phi_\parallel$ and the boundary values at s_2. We then specialize to an electron-ion plasma and impose the Q-N condition to solve for $\phi_\parallel$. Neglecting gravity, the solution is

$$w_{\alpha\perp}(s) = w_{\alpha\perp 2}[B(s)/B_2] \tag{25}$$

$$w_{\alpha\parallel}(s) = w_{\alpha\parallel 2} + w_{\alpha\perp 2}[1 - B(s)/B_2] + q_\alpha[\phi_{\parallel 2} - \phi_\parallel(s)] \tag{26}$$

$$u_\alpha(s) = u_{\alpha 2}[w_{\alpha\parallel}(s)/w_{\alpha\parallel 2}]^{1/2} \tag{27}$$

$$n_\alpha(s) = n_{\alpha 2}(B(s)/B_2)[w_{\alpha\parallel 2}/w_{\alpha\parallel}(s)]^{1/2} \tag{28}$$

$$\phi_\parallel(s) = \phi_{\parallel 2} + \left[\frac{w_{i\parallel 2}w_{e\perp 2} - w_{e\parallel 2}w_{i\perp 2}}{e(w_{i\parallel 2} + w_{e\parallel 2})}\right]\left[\frac{B(s)}{B_2} - 1\right] \tag{29}$$

where the subscript 2 denotes the value of the quantity at s_2 and e is the magnitude of the electronic charge. From (29), we see that $E_\parallel$ is

$$E_\parallel = -\,d\phi_\parallel/ds = -K\,dB/ds \tag{30}$$

$$K = \left(\frac{1}{eB_2}\right)\left[\frac{w_{i\parallel 2}w_{e\perp 2} - w_{e\parallel 2}w_{i\perp 2}}{w_{i\parallel 2} + w_{e\parallel 2}}\right]. \tag{31}$$

Equation (30) is the A–F formula for $E_\parallel$ for upward auroral-current regions and is identical to (12) of [3, Sec. 5.1.3], except that $w_{\alpha\parallel}$ has both a thermal part and a drift part, as $w_{\alpha\parallel} = T_{\alpha\parallel}/2 + m_\alpha u_\alpha^2/2$. It was derived in [3] by a different method, i.e., single-particle orbit theory, and applied for different boundary conditions. The boundary conditions used in [3] are that ionospheric ions are emitted at the lower boundary and magnetosperic electrons are injected at the upper boundary. For that problem, u_{i1} and hence u_{i2} are positive, and u_{e2} is negative. In this paper, we have applied the A–F formula to the problem where the ions and electrons are of magnetospheric origin and both are injected at the upper boundary, hence u_{i2} and u_{e2} are negative. Using (25), (26), and (29), we may also show that K is an invariant. Equation (30) is also equivalent to (28) obtained in [6] by using Persson's method of solution [4], [5]. As pointed out in [3], the differential particle anisotropy is such that $[w_{i\parallel 2}w_{e\perp 2} - w_{e\parallel 2}w_{i\perp 2}]$ is positive and, since dB/ds is negative, $E_\parallel$ is upward pointing.

A graph of the solution given by (25)–(30) is shown in Fig. 3, where s measures the distance along B from the surface of the earth. Remember that $w_{\alpha\perp} = T_{\alpha\perp}$. We have also plotted the current density, $j_\parallel$, which is defined as $j_\parallel = en(u_i - u_e)$. Here we have used the superscript M to denote the fact that the particles are of magnetospheric origin. In plotting the solution, we have imposed the following conditions. The physical conditions are $s_1 - s_0 = 1000$ km, $s_2 - s_0 = 6500$ km, $m_i/m_e = 250$, $B(s) = B_0(s_0/s)^3$, $B_0 = 0.57$ Gauss, where s_0, the radius of the earth, is approximated by 6400 km. The boundary conditions at s_2 are $n_{i2} = n_{e2} = n_2 = 0.50$ cm^{-3}, $u_{i2} = -5.6 \times 10^3$ km/s, $u_{e2} = -6.8 \times 10^3$ km/s, $T_{i\parallel 2} = T_{e\parallel 2} = T_{i\perp 2} = T_{e\perp 2} = 1.0$ keV, and $\phi_{\parallel 2} = -4.1 \times 10^3$ V. These parameters give $j_{\parallel 2} = 0.10\ \mu$A/m^2, $w_{i\parallel 2} = 22.4$ keV, and $w_{e\parallel 2} = 0.62$ keV. Since $\phi_\parallel$ is arbitrary to a constant, we have adjusted $\phi_{\parallel 2}$ so that $\phi_{\parallel 1} = 0$ for convenience in plotting. The mass and temperature ratios are unrealistic and the current density is too small. However, $w_{i\parallel 2} = 22.4$ keV is realistic for strong injection events [38]. We use these parameters in order to compare the A–F solution to Schriver's simulation [18] in Section II-D. In this example, since $w_{e\perp 2}$ is comparable to $w_{i\perp 2}$ and $w_{i\parallel 2} \gg w_{e\parallel 2}$, a good approximation for $\phi_\parallel$ is

$$\phi_\parallel(s) \cong \phi_{\parallel 2} + e^{-1}w_{e\perp 2}[\gamma(s) - 1] \tag{32}$$

where $\gamma(s) = B(s)/B_2$. For these conditions, the potential drop from s_1 to s_2 ($\phi_{\parallel 2} - \phi_{\parallel 1}$) scales as $w_{e\perp 2}$.

C. Self-Consistent Formulas for $E_\parallel$

Equations (15) and (16) give four self-consistent formulas for $E_\parallel$ in an electron-ion plasma. In order to verify the validity of these expressions, we use closure, substitute (25)–(29) into the right-hand sides of (15) and (16), and find that $E_\parallel$ is indeed given by (30).

Consider (15) for the ions. It is

$$E_\parallel = (2/e)\{-B^{-1}\,dB/ds[w_{i\parallel} - w_{i\perp}/2] + n_i^{-1}\,d/ds\,n_i w_{i\parallel}\}. \tag{33}$$

We wish to demonstrate that $E_\parallel$ is positive by using (33) and the results given in Fig. 3 instead of (30). To do this, we note that since $-B^{-1}\,dB/ds$ is positive and $w_{i\parallel} > w_{i\perp}/2$, then the first term on the right-hand side of (33) is positive. The second term is negative, but $|n_i^{-1}\,d/ds\,n_i w_{i\parallel}|$ is smaller than the first term inside the brackets, so $E_\parallel$ is positive. This is shown in Fig. 4, where $E_\parallel^{(1)}$ and $E_\parallel^{(2)}$ denote the first and second terms on the right-hand side of (33), respectively, and $E_\parallel^{(\text{total})}$ is the total $E_\parallel$. We see that once the solution is known, then the fact that $E_\parallel$ is positive can be seen from the ion moments alone.

D. Comparison to the Schriver Particle-in-Cell Simulation

In this section, we compare the A–F solution to the particle-in-cell (PIC) simulation in the electrostatic approximation given by Schriver [18]. The physical and boundary conditions that we chose in Section II-B are essentially identical to run number 3 in [18, Table 2], where u_i/v_{te} at s_2 is 0.3. In both cases, $u_{i2} = -5.6 \times 10^3$ km/s and $w_{i\parallel 2} = 22.4$ keV. The fact that $j_{\parallel 2}$ was 0.1 μA/m^2 in Section II-B and zero in the simulation makes little difference in the results.

As we saw in Section II-B, the A–F formula for $E_\parallel$ was obtained when the ionospheric particles and wave-particle interactions were neglected, the Q-N condition was used in place of Poisson's equation, and only the injected energetic magnetospheric particles were included. From [18, Fig. 5], we see that the potential drop is -2.7 kV compared to -4.1 kV from the A–F formula shown in Fig. 3, and that the shape of $\phi_\parallel(s)$ is concave downward ($d^2\phi_\parallel/ds^2 < 0$) instead of convex upward ($d^2\phi_\parallel/ds^2 > 0$) in the A–F formula. To find the polarization charge density, we may substitute $\phi_\parallel$ into Poisson's equation. We find that the shape of $\phi_\parallel$ in the simulation is consistent with the correct polarization charge density, whereas the A–F result is

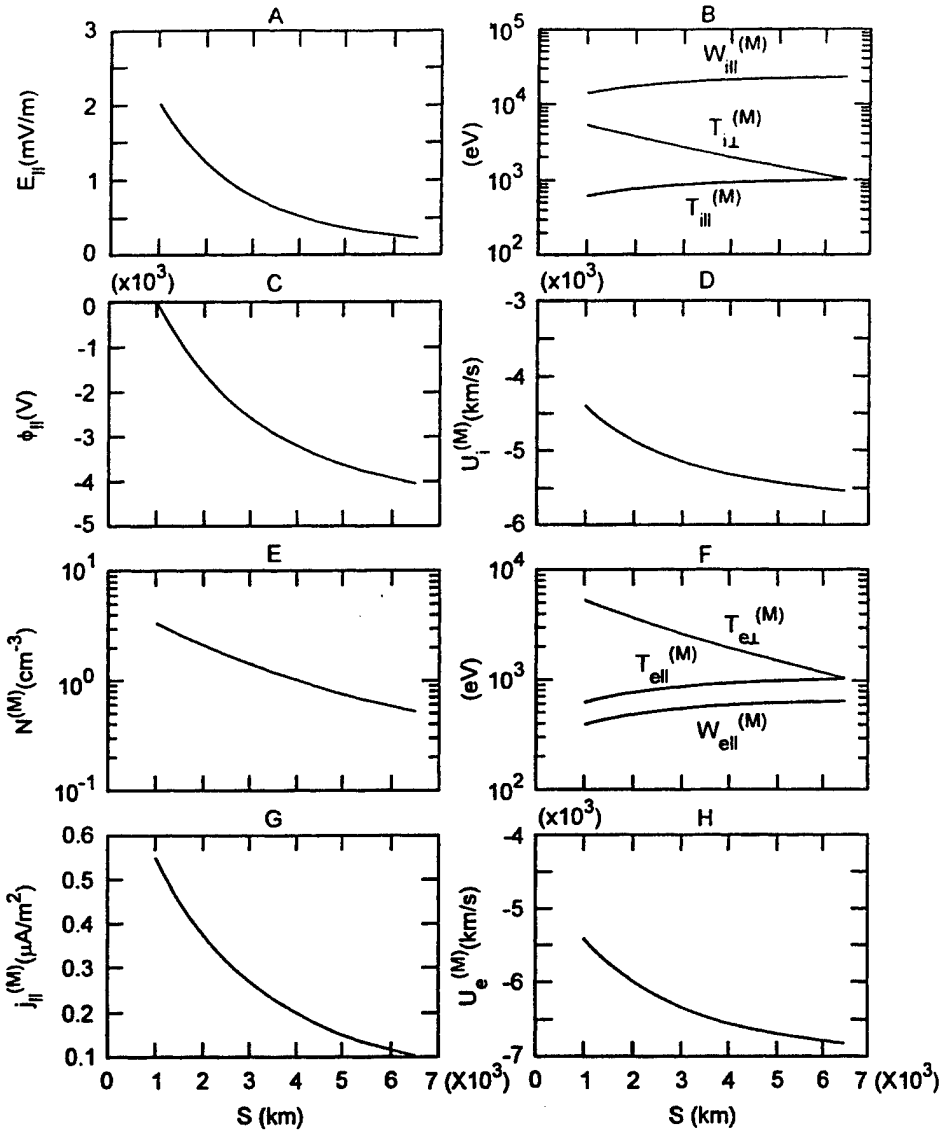

Fig. 3. The A–F solution for injected magnetospheric particles in an upward auroral-current region from (25)–(30). The symbols are defined in the text, and the superscript M denotes particles of magnetospheric origin.

not. Apparently, including ionospheric particles and wave-particle interactions, and using Poisson's equation instead of the Q-N condition, have modified the shape and magnitude of the potential drop.

However, it appears that the A–F formula gives the essential physics of the problem correctly, i.e., that for earthward-streaming energetic magnetospheric particles, it is the differential velocity-space anisotropy between the ions and the electrons that produces the potential drop and the upward pointing $E_{||}$.

III. Parallel E-Field Consistent with the Turbulent Heating of Ionospheric Ions in Downward Auroral-Current Regions

The purpose of this section is to give the analogue of the A–F formula for $E_{||}$ in downward auroral-current regions. For upward currents, $E_{||}$ is positive, as we saw in Section II; but for downward currents, $E_{||}$ is negative, as we will see in this section. We obtain this result by generalizing the method presented in Section II.

A. Kinetic Diffusion Equations and the Quasi-Neutrality Condition

Downward auroral-current regions are often characterized by energetic ion conics and upflowing, field-aligned electrons of ionospheric origin; intense broadband ELF (BBELF) electric-field turbulence; and small fluxes of earthward-streaming magnetospheric particles. The simplest model for downward auroral-current regions that we can think of is neglecting the magnetospheric particles and considering only the ionospheric particles and the BBELF turbulence. In this paper, we also assume

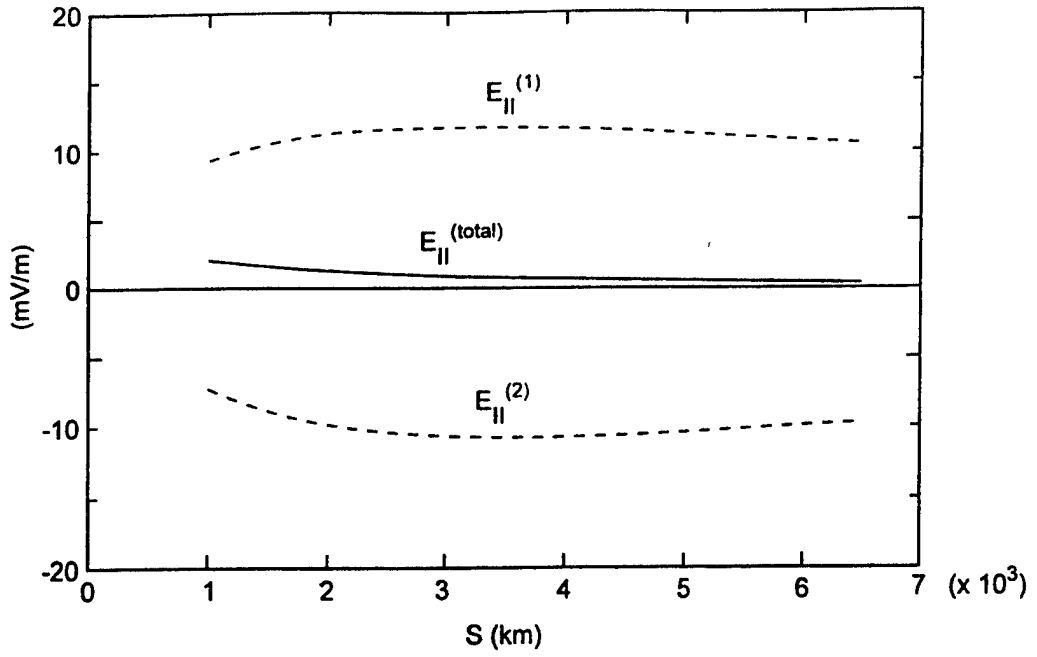

Fig. 4. The solution for $E_{||}$ in an upward auroral-current region from the self-consistent A–F formula for $E_{||}$ given by (33). Here, $E_{||}^{(1)}$ is the positive contribution, $E_{||}^{(2)}$ is the negative contribution, and $E_{||}^{(total)}$ is the total.

that the spectrum of the BBELF turbulence is given experimentally. How the turbulence is driven (or generated) is an active area of research and beyond the scope of this paper. If an additional source of ion heating exists on the flux tube due, for example, to the presence of fast bipolar solitary structures as suggested in [23] and [24], then see Section IV for a brief discussion of how this effect may be incorporated into the method of solution presented in this paper.

In Section II-C, we showed that a positive $E_{||}$ occurs when $w_{i||} > w_{i\perp}/2$ for the ions, and the magnitude of the second term in (33) is smaller than the first term. In Section III-C, we will show that a negative $E_{||}$ will occur when the reverse ion anisotropy is true, i.e., when $w_{i\perp}/2 > w_{i||}$, and certain other conditions are satisfied. Thus, in this section, we propose the following model for a negative $E_{||}$ in a quasi-stable downward auroral-current region: 1) the driver of the BBELF turbulence is unspecified, but the spectrum of the turbulence is given experimentally and 2) the self-consistent $E_{||}$ is sustained by a two-fold mechanism where the BBELF turbulence resonantly heats the ions perpendicular to B which, in a dipolar magnetic field, produces a velocity-space anisotropy in the ion distribution function where $w_{i\perp}/2 > w_{i||}$. Of course, the negative $E_{||}$ must also be self-consistent with the upward acceleration of the electrons, and this relationship is also discussed in Sections III-B and III-D.

The steady-state kinetic diffusion equations in one-spatial and two-velocity dimensions are

$$\left\{v_{||}\frac{\partial}{\partial s}+\left[g_{||}+\frac{q_\alpha}{m_\alpha}E_{||}\right]\frac{\partial}{\partial v_{||}} - \frac{1}{2B}\frac{dB}{ds}\left[v_\perp^2\frac{\partial}{\partial v_{||}}-v_{||}v_\perp\frac{\partial}{\partial v_\perp}\right]\right\}f_\alpha=\left(\frac{\delta f}{\delta t}\right)_\alpha \quad (34)$$

$$\left(\frac{\delta f}{\delta t}\right)_\alpha=\frac{1}{v_\perp}\frac{\partial}{\partial v_\perp}v_\perp D_{\alpha\perp}\frac{\partial}{\partial v_\perp}f_\alpha, \quad (35)$$

and the quasi-neutrality (Q-N) condition is

$$n_e=\sum_\beta n_\beta \quad (36)$$

where β is summed over the ions. Equations (34)–(36) are identical to (1) and (2) except for the velocity-space diffusion term. Here, $D_{\alpha\perp}$ is the perpendicular component of the gyrotropically averaged diffusion tensor, which is discussed below. Equation (34) has been used before to develop a kinetic theory of the "pressure cooker" effect in downward auroral-current regions [29], [30]. For the original reference on the "pressure cooker" effect, see [21].

As mentioned above, we assume that BBELF turbulence exists on the flux tube, is given experimentally, and that the waves heat the ions by cyclotron resonance near the ion gyrofrequency. Also, we do not specify the driver of the turbulence nor do we attempt a self-consistent treatment of the particles and the waves.

In general, the diffusion tensor for the problem contains both a perpendicular and a parallel part and is velocity dependent. It may be derived for electromagnetic modes from quasi-linear theory [39] or from Fokker–Planck theory by assuming that the particles undergo a random walk in velocity space [40]. If the dominant modes are electromagnetic and the ion energies are less than about 1 KeV, then $k_{||}v_{||} \ll \Omega_i$ and $D_\perp \gg D_{||}$, where $k_{||}$ is the parallel wave vector, Ω_i is the ion gyrofrequency, and $D_{||}$ is the parallel component of the diffusion tensor. For these conditions, the turbulent (anomalous), resonant perpendicular ion heating rate is

$$\dot{w}_{i\perp}=2m_iD_{i\perp}=(q_i^2/2m_i)S_L(\omega=\Omega_i) \quad (37)$$

where $S_L(\Omega_i)$ is the fraction of the total electric-field spectral density in the left-hand circular polarized (LHCP) electromagnetic ion cyclotron component and is velocity independent. This result may also be derived from simple arguments [41]. However, if the dominant modes are electrostatic, then the diffusion tensor for the problem contains velocity dependence, and (35) and (37) are approximate.

For the electrons, $D_{e\perp} \cong 0$, since there is no resonant heating at these low frequencies. However, preliminary studies show that under certain conditions, nonresonant wave-electron interactions are important. In this paper, we neglect all turbulent electron heating. Therefore, the approximation that we use is that the kinetic diffusion equation is used for the ion dynamics where only the perpendicular diffusion term is retained, and the Vlasov equation is used for the electron dynamics.

In (36), Poisson's equation has been replaced by the Q-N condition. The same remarks made in Section II-A about the validity of this replacement apply here.

B. Numerical Solution for $E_\parallel$ and Related Quantities from the Multimoment Fluid Equations

We now proceed to derive the multimoment fluid equations by multiplying (34) by $v_\perp^n v_\parallel^\ell$ and integrating over all velocity space. We use the same notation as in Section II-B. In addition, we need to evaluate the following integrals:

$$2\pi \int_{-\infty}^{\infty} dv_\parallel v_\parallel^\ell \int_0^\infty dv_\perp v_\perp^n \frac{\partial}{\partial v_\perp} v_\perp D_{\alpha\perp} \frac{\partial}{\partial v_\perp} f_\alpha.$$

Since $D_{\alpha\perp}$ depends only on s in our model, the integrals are zero for $n = 0$, are

$$D_{\alpha\perp} 2\pi \int_{-\infty}^{\infty} dv_\parallel v_\parallel^\ell \int_0^\infty dv_\perp f_\alpha = D_{\alpha\perp}\langle -1, \ell\rangle_\alpha$$

for $n = 1$ and $n^2 D_{\alpha\perp}\langle n-2, \ell\rangle_\alpha$ for $n \geq 2$. Using these definitions for the bracket symbols, the multimoment fluid equations for all n and ℓ are

$$\begin{aligned} &d/ds\langle n, \ell+1\rangle_\alpha + \dot{A}(1+n/2)\langle n, \ell+1\rangle_\alpha \\ &\quad + \ell\{(q_\alpha/m_\alpha)(d/ds\Phi_{\alpha\parallel})\langle n, \ell-1\rangle_\alpha \\ &\quad - (\dot{A}/2)\langle n+2, \ell-1\rangle_\alpha\} \\ &\quad = n^2 D_{\alpha\perp}\langle n-2, \ell\rangle_\alpha. \end{aligned} \tag{38}$$

Using the same definitions and procedures as in Section II, we find that the multimoment fluid equations for $n = 0$, $\ell = 0$; $n = 0$, $\ell = 1$; $n = 0$, $\ell = 2$; and $n = 2$, $\ell = 0$ are

$$B\, d/ds(n_\alpha u_\alpha/B) = 0 \tag{39}$$

$$\begin{aligned} &d/ds(n_\alpha w_{\alpha\parallel}) - B^{-1}\, dB/ds\, n_\alpha(w_{\alpha\parallel} - w_{\alpha\perp}/2) \\ &\quad + n_\alpha(q_\alpha/2)\, d/ds\, \Phi_{\alpha\parallel} = 0 \end{aligned} \tag{40}$$

$$\begin{aligned} &B\, d/ds\{[n_\alpha Q_{\alpha\parallel} + n_\alpha Q_{\alpha\perp} + q_\alpha n_\alpha u_\alpha \Phi_{\alpha\parallel}]/B\} \\ &\quad = \dot{w}_{\alpha\perp} n_\alpha \end{aligned} \tag{41}$$

$$B^2\, d/ds(n_\alpha Q_{\alpha\perp}/B^2) = \dot{w}_{\alpha\perp} n_\alpha. \tag{42}$$

Equations (39)–(42) are the standard balance equations for the number flux, momentum, total energy flux, and perpendicular energy flux, respectively.

As in Section II, formal expressions for $E_\parallel$ may be found from (40) and (41). Neglecting gravity, we have

$$\begin{aligned} E_\parallel &= (2/q_\alpha)\{B^{-1}\, dB/ds(w_{\alpha\perp}/2 - w_{\alpha\parallel}) \\ &\quad + n_\alpha^{-1}\, d/ds\, n_\alpha w_{\alpha\parallel}\} \end{aligned} \tag{43}$$

$$\begin{aligned} E_\parallel &= -(q_\alpha u_\alpha)^{-1}\dot{w}_{\alpha\perp} + (B/q_\alpha n_\alpha u_\alpha)\, d/ds \\ &\quad \cdot [(n_\alpha Q_{\alpha\parallel} + n_\alpha Q_{\alpha\perp})/B]. \end{aligned} \tag{44}$$

These are the self-consistent formulas for $E_\parallel$ which must be satisfied once the solution for the problem is found.

In order to solve (39)–(42) and (36), we must introduce closure approximations. Instead of using the standard procedure, we introduce the same closure assumptions which we did in Section II-B by imposing (17) and (18). Using (17), (18), and (39), we see that the multimoment fluid equations become

$$d/ds(n_\alpha u_\alpha/B) = 0 \tag{45}$$

$$\begin{aligned} &d/ds\, n_\alpha w_{\alpha\parallel} - B^{-1}\, dB/ds\, n_\alpha[w_{\alpha\parallel} - w_{\alpha\perp}/2] \\ &\quad + n_\alpha(q_\alpha/2)\, d/ds\, \Phi_{\alpha\parallel} = 0 \end{aligned} \tag{46}$$

$$d/ds(w_{\alpha\parallel} + w_{\alpha\perp} + q_\alpha\Phi_{\alpha\parallel}) = \dot{w}_{\alpha\perp}/u_\alpha \tag{47}$$

$$B\, d/ds(w_{\alpha\perp}/B) = \dot{w}_{\alpha\perp}/u_\alpha \tag{48}$$

$$n_e = \sum_\beta n_\beta, \qquad \beta = \text{ions}. \tag{49}$$

Equations (45)–(49) are a set of $4\alpha + 1$ nonlinear, first-order ordinary differential equations for $4\alpha + 1$ unknowns subject to boundary conditions imposed at either end of the flux tube. With the aid of (45), we may show that as $T_{i\parallel} \to 0$, (47) and (48) for the ions reduce to the ion mean particle equations of motion given in [21] and [41].

The same remarks about this closure assumption made in Section II-B apply here. Basically, this closure amounts to the assumption that $T_{\alpha\parallel}$ and $m_\alpha u_\alpha^2$ change proportionately from s_1 to s_2, so that the ratio $(T_{\alpha\parallel}/2 + m_\alpha u_\alpha^2/2)/(m_\alpha u_\alpha^2/2)$ is nearly constant. We have examined some S3-3 [21], FREJA [22], and FAST [23] ion and electron particle data for downward auroral-current regions. We find that the ion conic data at the satellite altitude show distributions where both $T_{i\parallel}$ and $m_i u_i^2$ have increased more or less proportionately from their ionospheric boundary values. The satellite data also show "flat top" or "cigar shaped" electron distribution functions for downward auroral-current regions where a similar statement about $T_{e\parallel}$ and $m_e u_e^2$ is true. For these reasons, we argue that the closure we use is approximately valid for downward auroral-current regions.

Before we are able to solve the multimoment fluid equations, we must specify the turbulent, resonant perpendicular ion heating rate, $\dot{w}_{i\perp}$, and the boundary conditions. In this section, we impose conditions consistent with the FREJA experimental observations by Boehm *et al.* [22] for a downward auroral-current region. We do this so that we may compare the theoretical results to the experimental results in Section III-E. In that data set, the total electric-field spectral density, $S(f)$, was measured at the satellite altitude [22]. In the vicinity of the oxygen cyclotron frequency, we found that $S(f) \sim f^{-\alpha}$. Since S is evaluated at $f = f_i$, this leads to

$$S_L(f = f_i) = \eta_L S_o(s/s_o)^{3\alpha} \tag{50}$$

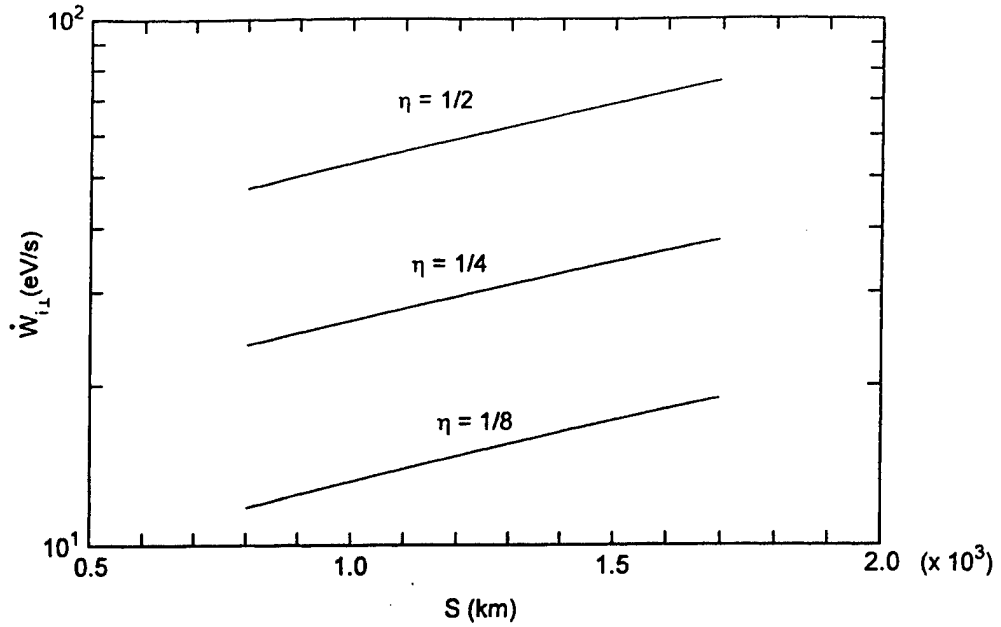

Fig. 5. The turbulent (anomalous), resonant perpendicular ion heating rate for $\eta_L = 1/2, 1/4$, and $1/8$ from (37).

where

- s_o the radius of the earth, is approximated by 6400 km;
- η_L is the fraction of the total spectral power in the LHCP ion cyclotron component; and
- α is the spectral index.

For this data set, we found that $S_o = 2 \times 10^{-5}$ (V/m)^2(Hz)$^{-1}$ and $\alpha = 1.3$. Since no information was available about the altitude dependence of S_0, we assumed it to be uniform. In Fig. 5, we show a graph of $\dot{w}_{i\perp}$ versus s for $\eta_L = 1/2, 1/4$, and $1/8$. We see that as the ions are heated and move up the B-field line, the heating rate increases because the ions are in resonance with lower and lower frequencies. We also assume that the dominant ion was atomic oxygen and that $s_1 - s_o = 800$ km, $s_2 - s_o = 1700$ km (the satellite altitude), $B(s) = B_o(s_o/s)^3$, and $B_o = 0.57$ Gauss. The boundary conditions at s_1 are $n_{i1} = n_{e1} = n_1 = 10^3$ cm^{-3}, $u_{i1} = 0.5$ km/s, $u_{e1} = 15$ km/s, $T_{i\parallel 1} = T_{i\perp 1} = 0.1$ eV, $T_{e\parallel 1} = T_{e\perp 1} = 0.3$ eV, and $\phi_{\parallel 1} = 0$. These parameters give $j_{\parallel 1} = -2.3$ μA/m^2, $w_{i\parallel 1} = 0.071$ eV, and $w_{e\parallel 1} = 0.151$ eV, and are typical for the topside, high-latitude ionosphere [42].

We now proceed to solve (45)–(49) by a numerical method. The method finds the $4\alpha + 1$ values of n_α, u_α, $w_{\alpha\parallel}$, $w_{\alpha\perp}$, and $\phi_\parallel$ as a function of s given their values at one boundary. In this case, $s_1 \leq s \leq s_2$, and the boundary is s_1. The procedure implements the semi-implicit discretization method of Bader and Deuflhard [43] and works for nonlinear systems of first-order differential equations that may be stiff. The method was tested by setting $\dot{w}_{i\perp}$ very small and thereby obtaining the analytical results given in Section II-B for those boundary conditions. A graph of the numerical solution is given in Fig. 6, where we have chosen $\eta_L = 1/2$ and where s measures the distance along B from the surface of the earth. Remember that $w_{\alpha\perp} = T_{\alpha\perp}$. We have also plotted the current density $j_\parallel$. Here, we have used the superscript I to denote the fact that the particles are of ionospheric origin. The dashed curve in the $n^{(I)}$ graph gives the density of the background ionosphere when there is no turbulent perpendicular ion heating, i.e., when $\dot{w}_{i\perp} = 0$. We note here that there is a predicted potential increase of 610 V from 800 to 1700 km for the Boehm *et al.* data set.

In Sections III-C–III-E, we will discuss further aspects of the solution shown in Fig. 6. However, we wish to say here that the major point of this paper is that for downward auroral-current regions, $E_\parallel$ is negative and there is a potential increase from the ionosphere to the magnetosphere. This is opposite to the result for upward auroral-current regions, where the A–F formula gives $E_\parallel$ positive and a potential drop from the ionosphere to the magnetosphere. We also note here that $\phi_\parallel$ is concave upward ($d^2\phi_\parallel/ds^2 > 0$) and that the polarization charge density found from Poisson's equation has the correct sign for a negative $E_\parallel$ region.

C. Analogue for the A–F Formula for $E_\parallel$ in Downward Auroral-Current Regions

Equations (43) and (44) give four self-consistent formulas for $E_\parallel$ in an electron-ion plasma. If we had an analytic solution of the problem, we could substitute it into any one of these expressions and get the correct formula for $E_\parallel$. Since we do not, we may substitute the numerical solution into these equations in order to understand how a negative $E_\parallel$ is sustained in downward auroral-current regions.

For example, consider (43) for the ions. It is

$$E_\parallel = (2/e)\{B^{-1}\, dB/ds(w_{i\perp}/2 - w_{i\parallel}) + n_i^{-1}\, d/ds\, n_i w_{i\parallel}\}. \quad (51)$$

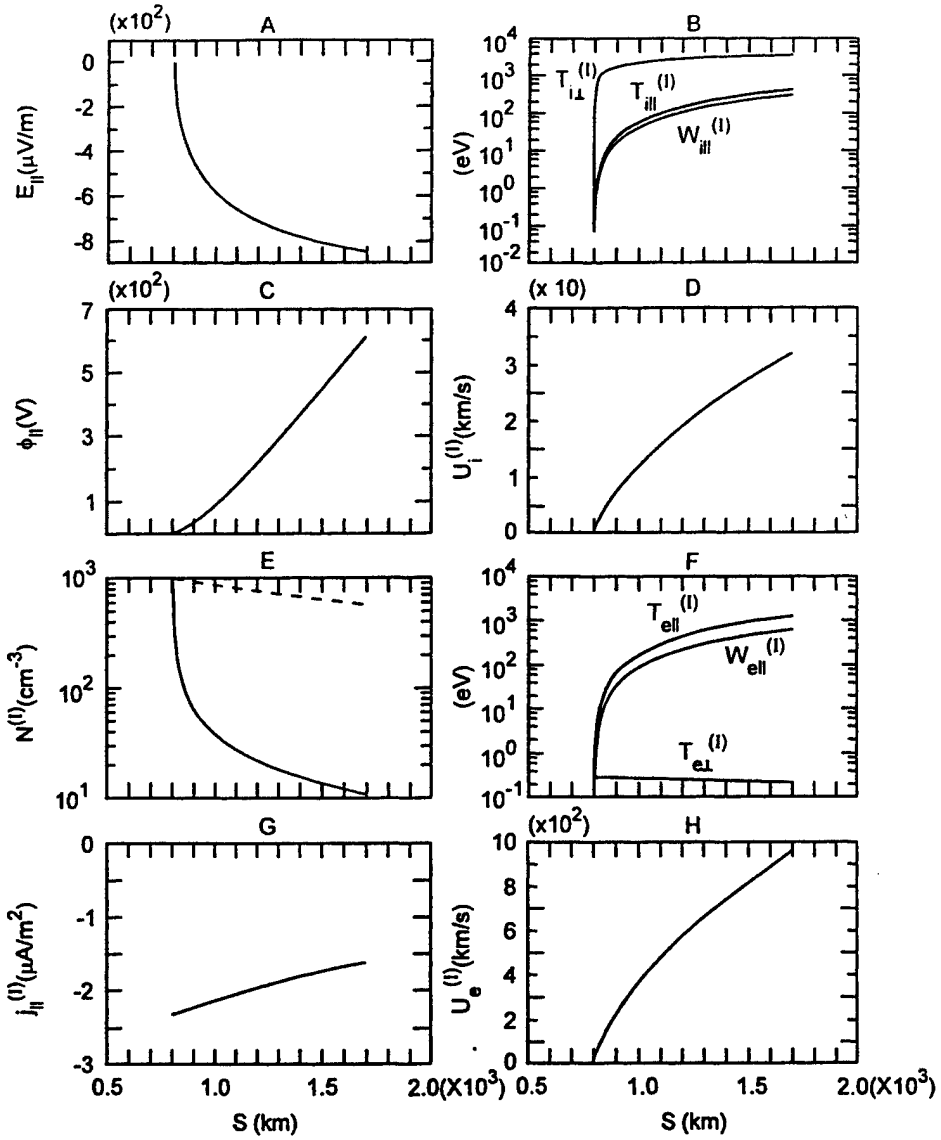

Fig. 6. The numerical solution for the turbulent (anomalous) heating of ionospheric ions in a downward auroral-current region observed by the FREJA satellite from (45)–(49). The symbols are defined in the text, $\eta_L = 1/2$, and the superscript I denotes particles of ionospheric origin.

We may integrate (48) from s_1 to s to obtain a formal expression for $w_{i\perp}$

$$w_{i\perp}(s) = \left[\frac{B(s)}{B_1}\right] w_{i\perp 1} + B(s) \int_{s_1}^{s} ds' \left[\frac{\dot{w}_{i\perp}(s')}{B(s')u_i(s')}\right]. \tag{52}$$

Now we can see what is happening in (51). If the turbulent perpendicular ion-heating rate is sufficiently large, then $w_{i\perp}/2 - w_{i\parallel}$ is positive (see Fig. 6) and, since $B^{-1}\, dB/ds$ is negative, the first term on the right-hand side of (51) is negative. From Fig. 6, we also see that $n_i^{-1}\, d/ds\, n_i w_{i\parallel}$ is positive, but smaller than the magnitude of the first term of (51) inside the brackets. Therefore, $E_\parallel$ is negative. This is shown in Fig. 7, where $E_\parallel^{(1)}$ and $E_\parallel^{(2)}$ denote the first and second terms on the right-hand side of (51), respectively, and $E_\parallel^{(\text{total})}$ is the total $E_\parallel$. We see that once the numerical solution is known, then the fact that $E_\parallel$ is negative can be understood from the ion moments alone.

For comparative purposes, we will refer to (51) and (52) as the analogue of the A–F formula for $E_\parallel$ in downward auroral-current regions. Although (51) is formally the same as (33) in Section II-C, its physical content is different. For downward auroral-current regions, it is the turbulent, resonant perpendicular ion heating that produces the ion temperature anisotropy ($w_{i\perp}/2 > w_{i\parallel}$) which is consistent with the negative $E_\parallel$. Since upward and downward auroral-current regions have opposite ion velocity-space anisotropies, their parallel E-fields have opposite signs.

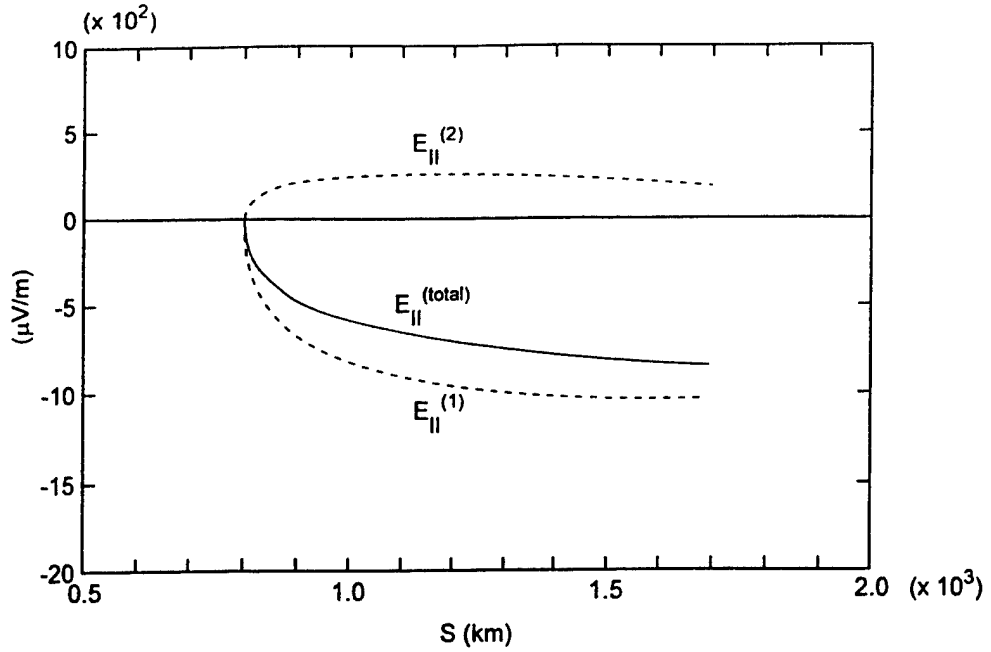

Fig. 7. The solution of the analogue of the A–F formula for $E_\parallel$ in a downward auroral-current region given by (51). Here, $E_\parallel^{(1)}$ is the negative contribution, $E_\parallel^{(2)}$ is the positive contribution, and $E_\parallel^{(\mathrm{total})}$ is the total.

D. Understanding the Behavior of the Solution

In Section III-C, we gave what we call an analogue of the A–F formula for $E_\parallel$ in downward auroral-current regions and a condition on the moments of the ion distribution function which is self-consistent with the negative $E_\parallel$. Now, we wish to give a physical interpretation of the behavior of the ion and electron moments shown in Fig. 6, using the conservation relations.

In order to understand the behavior of $T_{i\perp}$ and $T_{e\perp}$, we recall that $w_{\alpha\perp} = T_{\alpha\perp}$ and use perpendicular energy balance (48). For the ions, we have

$$d/ds(T_{i\perp}/B) = \dot{w}_{i\perp}/u_i B. \tag{53}$$

Since $\dot{w}_{i\perp}/u_i B$ is positive, $T_{i\perp}/B$ increases with s in such a way that $T_{i\perp}$ increases from its boundary value of 0.1 eV at 800 km to 3.4 keV at 1700 km. If other perpendicular ion heating processes operate on the flux tube due, for example, to the presence of fast bipolar solitary structures, then the heating rate for that process may be added to $\dot{w}_{i\perp}$. The amount of perpendicular ion heating would then be increased from that produced by the BBELF turbulence alone. For the electrons, $\dot{w}_{e\perp}$ is zero, so

$$d/ds(T_{e\perp}/B) = 0 \tag{54}$$

and $T_{e\perp}$ cools adiabatically from its boundary value of 0.3 eV at 800 km to 0.21 eV at 1700 km. If other electron heating processes operate on the flux tube, this result could be modified.

We saw in Section III-C that when $\dot{w}_{i\perp}$ is sufficiently large, it dominates the particle dynamics and the gravitational potential can be neglected compared to the electrostatic potential. Under these conditions, consider total energy balance (47) for the electrons. Since $d/ds\ w_{e\perp}$ is small compared to $d/ds\ w_{e\parallel}$, we may neglect it to find that

$$d/ds\ w_{e\parallel} = d/ds[T_{e\parallel}/2 + m_e u_e^2/2] \cong -eE_\parallel. \tag{55}$$

Since $E_\parallel$ is negative, $w_{e\parallel}$ increases with s from its boundary value of 0.15 eV at 800 km to 610 eV at 1700 km. We see that it is the downward-pointing $E_\parallel$ that is self-consistent with the upward acceleration of the electrons. Because of the closure assumption, which is consistent with the electron experimental data, $w_{e\parallel}$ is partitioned proportionately between the thermal part and the drift part so that both increase with s. Equation (55) may be integrated from s_1 to s to obtain an approximate conservation relation for $\phi_\parallel$ and $w_{e\parallel}$.

$$e[\phi_\parallel(s) - \phi_\parallel(s_1)] \cong w_{e\parallel}(s) - w_{e\parallel}(s_1). \tag{56}$$

It is interesting to consider the more rigorous conservation of total energy flux for the electrons from (41) before any closure approximation is made. Since $d/ds\ n_e Q_{e\perp}$ is small compared to $d/ds\ n_e Q_{e\parallel}$ and the gravitational potential may be neglected compared to the electrostatic potential, we obtain

$$d/ds\{(n_e u_e/B)[n_e Q_{e\parallel}/n_e u_e - e\phi_\parallel]\} \cong 0. \tag{57}$$

Using (39), we may simplify this expression and integrate from s_1 to s to obtain

$$e[\phi_\parallel(s) - \phi_\parallel(s_1)] \cong E_0(s) - E_0(s_1) \tag{58}$$

where E_0 is the characteristic energy and is defined as $n_e Q_{e\parallel}/n_e u_e$. This is just the conservation relation calculated from the experimental data for downward auroral-current regions discussed and illustrated in Fig. 2 of Carlson *et al.* [23]. When we compare (56) to (58), we see that our closure approximation is valid for electron distributions that are more

beam-like than thermal-like and therefore underestimates the value of $\phi_\parallel$ compared to the more rigorous result given by (58).

Consider total energy balance (47) for the ions, where the gravitational potential may be neglected compared to the electrostatic potential

$$d/ds[T_{i\parallel}/2 + m_i u_i^2/2] + d/ds\, T_{i\perp} + e\, d/ds\, \phi_\parallel = w_{i\perp}/u_i. \tag{59}$$

From Figs. 5 and 6, we find that $w_{i\perp}/u_i$ is larger than $e\ d/ds\ \phi_\parallel$, which is positive. Therefore, the perpendicular wave-ion heating rate supplies the energy to heat the ions perpendicular to B and causes the ions to be heated and accelerated parallel to B, as shown in (59). Because of the closure assumption, which is consistent with both the ion conic data and the kinetic solution for the ion "pressure cooker" effect [29], $w_{i\parallel}$ is partitioned proportionately between the thermal part and the drift part so that both increase with s.

The rapid decrease of n can be understood from conservation of number flux (45)

$$d/ds(nu_a/B) = 0. \tag{60}$$

Since u_i and u_e both increase with s and B decreases with s, then n decreases rapidly from 10^3 cm^{-3} at 800 km to 11 cm^{-3} at 1700 km. This produces a cavity in the downward auroral-current region. For comparative purposes, the dashed curve in Fig. 6 gives the background value of n when there is no turbulent ion heating.

The current density

$$j_\parallel = en(u_i - u_e) \cong -enu_e \tag{61}$$

is dominated by the electron drift and is therefore downward-pointing.

E. Comparison to a FREJA Satellite Observation of a Downward Auroral-Current Region

In this section, we compare the theoretical results given in Section III-B to the experimental results of Boehm *et al.* [22] for a FREJA satellite pass through a downward auroral-current region near 1700 km in the morning auroral zone. In the Boehm *et al.* data set, the total electric-field spectral density, $S(f)$, was determined experimentally at the satellite altitude and is given in Section III-B. In the theory we present, there is one adjustable parameter, η_L, which we have chosen as 1/2. Also, we assume typical values [42] for the electron and ion moments at the lower boundary, which we chose to be 800 km. A comparison between the theoretical and experimental values for the quantities determined by the satellite at 1700 km is shown in Table I. The experimental values are taken from [22] where u_e was estimated using the formula $j_\parallel \cong -enu_e$, and θ is the ion conic angle. The other theoretical quantities at 1700 km may be determined from Fig. 6. We see reasonable agreement for all values given in the table with the possible exception of $T_{i\perp}$. However, the estimated experimental value of 5 keV is probably too large, and a more realistic range is from 2 to 3 keV. It is important to note that using the experimental value for u_e of 940 km/s, we find that the drift part of $w_{e\parallel}$ is 2.5 eV at 1700 km. From data shown in [22, Fig. 1], we also find that $T_{e\parallel}/2 \gg m_e u_e^2/2$ at the satellite altitude. Apparently, the electrons do not run away in an $E_\parallel$ field as a beam, but appear as a field-aligned distribution with a large $T_{e\parallel}/2$ compared to $m_e u_e^2/2$. This is also what is observed by the FAST satellite [23]. As pointed out in [22], this is probably due to strong wave-electron interactions. It is important to note here that wave-electron interactions are not taken into account in the present version of our theory, since we use the Vlasov equation for the electron dynamics. Instead, the experimental fact that $T_{e\parallel}/2 \gg m_e u_e^2/2$ is modeled by the electron closure approximation that we use.

IV. Discussion

In this paper, we give an alternative derivation of the A–F formula for a positive $E_\parallel$ in upward auroral-current regions [see (30)], and propose an analogous formula for a negative $E_\parallel$ in downward auroral-current regions [see (51) and (52)]. In addition, we derive a third result, i.e., an equivalent expression for the A–F formula for $E_\parallel$ in terms of the ion moments alone [see (33)].

The A–F formula is a benchmark result not only for pedagogical reasons (it is a closed-form solution), but also because it clarifies the essential physics of a particular model for auroral arc formation. In that model, the driver is the earthward-streaming, energetic magnetospheric particles, and the mechanism for sustaining a positive $E_\parallel$, thereby accelerating the auroral particles, is the differential velocity-space anisotropy between the ions and the electrons in the dipolar magnetic field ($w_{i\parallel 2} w_{e\perp 2} - w_{e\parallel 2} w_{i\perp 2} > 0$). Another way of looking at this result, in terms of the ion moments alone, reveals that $E_\parallel$ is positive when $w_{i\parallel} > w_{i\perp}/2$ and certain other conditions are met. According to the PIC simulation by Schriver, when ionospheric particles and wave-particle interactions in the electrostatic approximation are included in the model, the potential drop is reduced from its A–F value, and the shape of $\phi_\parallel$ is modified. In his review, Borovsky [17] identifies ten drivers and 12 possible mechanisms, none of which appears to explain all aspects of auroral arc formation. It is clear that more analytical and simulational work on upward auroral-current regions is needed.

The primary result that we present in this paper is a model for a negative $E_\parallel$ in downward auroral-current regions. The BBELF turbulence, which experiment shows is present, plays a central role. The driver of the turbulence is unspecified, but the spectrum of the turbulence is given experimentally. The self-consistent $E_\parallel$ is sustained by a two-fold mechanism where the BBELF turbulence resonantly heats the ions transverse to B which, in a dipolar magnetic field, produces an ion velocity-space anisotropy where $w_{i\perp}/2 > w_{i\parallel}$ [see (51) and (52)]. This is just the reverse anisotropy from that which occurs in the equivalent A–F formula for the ions [see (33)] and is consistent with an $E_\parallel$ of the opposite sign. Of course, $E_\parallel$ and hence $\phi_\parallel$ must also be self-consistent with the upward acceleration of the electrons [see (56) and the more rigorous expression given by (58)]. In this paper, we do not attempt to resolve how the downward auroral-current region is driven. This subject is an active area of research and beyond the scope of the present work. For example, the BBELF could be driven by the electron beam, shear in the two-dimensional ion flow, or some other mechanism. Whatever the case may be, the conservation laws derived

TABLE I
THEORY-DATA COMPARISON FOR A DOWNWARD AURORAL-CURRENT REGION

Quantity at 1700 km	Theory	FREJA Data
n (cm^{-3})	11	~10
u_e (km/s)	955	~940
$j_\parallel$ (μA/m^2)	-1.6	~ -1.5
$T_{e\perp}$ (eV)	0.21	0.1 - 0.25
$T_{i\perp}$ (keV)	3.4	< 5
$\Delta\phi_\parallel$ (Volts)	610	~700
θ (degrees)	106	100 - 110

from the appropriate kinetic model impose powerful constraints on the moments of the electron and ion distribution functions, the strength of the BBELF turbulence, and the magnitude and direction of $E_\parallel$. These conservation relations were discussed in Sections III-B and III-D. The central point of this paper is that both the velocity-space anisotropy of the particles and the turbulent heating of the ions play an important role in downward auroral-current regions.

When this model for downward auroral-current regions is applied to the FREJA data set by Boehm *et al.* [22] in the morning auroral zone, good agreement between theory and experiment is achieved (see Table I). For example, we find that $j_\parallel \sim -1.6$ μA/m^2 at 1700 km, the average parallel E-field $\langle E_\parallel \rangle \sim -680$ μV/m, and a potential increase of ~610 V from 800 to 1700 km are obtained. In [29] and [30], a kinetic theory of the "pressure cooker" effect was given for the S3-3 data set of Gorney *et al.* [21] using (34)–(36) for a downward auroral-current region in the dayside auroral zone. Again, good agreement between theory and experiment was achieved. Since the turbulence was weaker than that in the FREJA data, we found that $j_\parallel \sim -0.4$ μA/m^2 at 6000 km, $\langle E_\parallel \rangle \sim -12$ μV/m, and a potential increase of ~55 V from 1500 to 6000 km were obtained. In the anomalous transport calculation for the current-driven ion cyclotron instability reported in [26], they found that $j_\parallel \sim -1.1$ μA/m^2 and $\langle E_\parallel \rangle \sim -0.1$ μV/m for a 1 V potential increase in 10^4 km. This result for $\langle E_\parallel \rangle$ appears to be too small to be of significance in downward auroral-current regions.

The model presented here for downward auroral-current regions needs to be generalized. There is the obvious need to identify the driver of the BBELF turbulence and to treat the wave-particle interactions self-consistently. Aside from this, there are other, more straightforward generalizations that can be carried out. Recently, we have generalized this work in two ways. In addition to the presence of the heated and accelerated ionospheric particles, we have included a magnetospheric population of earthward-streaming ions and electrons. We find that as the flux of the magnetospheric particles is increased, a positive contribution to $E_\parallel$ is produced, and the total $E_\parallel$ is less negative. In fact, if the flux of magnetospheric particles is large enough, the two effects combine to produce a positive $E_\parallel$ and an upward auroral-current situation. A second way in which we have generalized the model is to include wave-particle interactions in the equation for the electrons. The BBELF waves cannot heat the electrons perpendicular to B by a cyclotron resonant interaction because the frequencies are too low, but there is a nonresonant diffusion process which acts parallel to B. Preliminary results indicate that this diffusion process spreads out the electron distribution function in velocity space parallel to B, prevents the formation of a runaway electron beam, and maintains a parallel electron energy, $w_{e\parallel}$, where $T_{e\parallel}/2 > m_e u_c^2/2$.

It should be mentioned here that there are processes other than ion cyclotron resonance with broadband waves by which ions can be heated in space plasmas. For a discussion of these processes, see [44]. Recently, a new process has been proposed based on an analysis of FAST data. The data show that within a broad region of downward auroral current, there are narrow subregions where intense bursts of fast bipolar solitary structures occur. These subregions coincide with enhanced ion heating (see [24, Fig. 1]). It has been pointed out [23] that the random pulses in the perpendicular E-field of the solitary structures as they propagate past the nearly stationary ions, could lead to a significant amount of stochastic ion heating. If a perpendicular ion heating rate can be calculated for this process, then it may be added to $\dot{w}_{i\perp}$ in (41) and (42). The resulting multimoment fluid equations may then be solved using the same method as presented in Section III-B. This would lead to an enhanced amount of perpendicular ion heating, as indicated in [24, Fig. 1].

ACKNOWLEDGMENT

The authors are indebted to M. Boehm for supplying details on the FREJA data set discussed in Section III. They also acknowledge important conversations with M. Boehm, T. Chang, J. Lemaire, W. Lennartsson, D. Schriver, and M. Schulz.

REFERENCES

[1] T. Iijima and T. A. Potemra, "Large-scale characteristics of field-aligned currents associated with substorms," *J. Geophys. Res.*, vol. 83, no. A2, pp. 599–615, 1978.
[2] R. C. Elphic *et al.*, "The auroral current circuit and field-aligned currents," *Geophys. Res. Lett.*, vol. 25, no. 12, pp. 2033–2036, 1998.
[3] H. Alfvén and C. G. Fälthammar, *Cosmical Electrodynamics*. Oxford, U.K.: Oxford Univ. Press, 1963, ch. 5.
[4] H. Persson, "Electric field along a magnetic field line of force in a low-density plasma," *Phys. Fluids*, vol. 6, no. 12, pp. 1756–1759, 1963
[5] ——, "Electric field parallel to the magnetic field in a low-density plasma," *Phys. Fluids*, vol. 9, no. 6, pp. 1090–1098, 1966.
[6] D. P. Stern, "One-dimensional models of quasi-neutral parallel electric fields," *J. Geophys. Res.*, vol. 86, no. A7, pp. 5839–5860, 1981.
[7] F. S. Mozer, C. A. Cattell, M. K. Hudson, R. L. Lysak, M. Temerin, and R. B. Torbeert, "Satellite measurements and theories of low altitude auroral particle acceleration," *Space Sci. Rev.*, vol. 27, pp. 155–213, 1980.
[8] R. Lundin, G. Haerendel, and S Grahn, "The FREJA project," *Geophys. Res. Lett.*, vol. 21, no. 17, pp. 1823–1826, 1994.
[9] C. W. Carlson, R. F. Pfaff, and J. G. Watzin, "The fast auroral snapshot (FAST) mission," *Geophys. Res. Lett.*, vol. 25, no. 12, pp 2013–2016, 1998.
[10] R. F Benson and W. Calvert, "ISIS 1 observations at the source of auroral kilometric radiation," *Geophys. Res. Lett.*, vol 6, no. 6, pp. 479–482, 1979.
[11] L. R. Lyons and D. S. Evans, "An association between discrete aurora and energetic particle boundaries," *J Geophys. Res* , vol 89, no. A4, pp 2395–2400, 1984.

[12] D. A. Gurnett, R. L. Huff, J. D. Menietti, J. L. Burch, J. D. Winningham, and S. D. Shawhan, "Correlated low-frequency electric and magnetic noise along the auroral field lines," *J. Geophys. Res.*, vol. 89, no. A10, pp. 8971–8985, 1984.

[13] C. S. Lin, J. N. Barfield, J. L. Burch, and J. D. Winningham, "Near-conjugate observations of inverted-V electron precipitation using DE-1 and DE-2," *J. Geophys. Res.*, vol. 90, no. A2, pp. 1669–1681, 1985.

[14] R. E. Erlandson, L. J. Zanetti, M. H. Acuna, A. I. Eriksson, L. Eliasson, M. H. Boehm, and L. G. Blomberg, "FREJA observations of electromagnetic ion cyclotron ELF waves and transverse oxygen ion acceleration on auroral field lines," *Geophys. Res. Lett.*, vol. 21, no. 17, pp. 1855–1858, 1994.

[15] F. S. Mozer, R. Ergun, M. Temerin, C. Cattell, J. Dombeck, and J. Wygant, "New features of time domain electric-field structures in the auroral acceleration region," *Phys. Rev. Lett.*, vol. 79, no. 7, pp. 1281–1284, 1997.

[16] J. P. McFadden *et al.*, "Spatial structure and gradients of ion beams observed by FAST," *Geophys. Res. Lett.*, vol. 25, no. 12, 1998.

[17] J. E. Borovsky, "Auroral arc thickness as predicted by various theories," *J. Geophys. Res.*, vol. 98, no. A4, pp. 6101–6138, 1993.

[18] D. Schriver, "Particle simulation of the auroral zone showing parallel electric fields, waves, and plasma acceleration," *J. Geophys. Res.*, vol. 104, no. A7, pp. 14655–14670, 1999.

[19] D. M. Klumpar and W. J. Heikkila, "Electrons in the ionospheric source cone: Evidence for runaway electrons as carriers of downward Birkeland currents," *Geophys. Res. Lett.*, vol. 9, no. 8, pp. 873–876, 1982.

[20] J. L. Burch, P. H. Reiff, and M. Sugiura, "Upward electron beams measured by DE-1: A primary source of dayside region-1 Birkeland currents," *Geophys. Res. Lett.*, vol. 10, no. 8, pp. 753–756, 1983.

[21] D. J. Gorney, Y. T. Chiu, and D. R. Croley, "Trapping of ion conics by downward parallel electric fields," *J. Geophys. Res.*, vol. 90, no. A5, pp. 4205–4210, 1985.

[22] M. H. Boehm *et al.*, "Observations of an upward-directed electron beam with the perpendicular temperature of the cold ionosphere," *Geophys. Res. Lett.*, vol. 22, no. 16, pp. 2103–2106, 1995.

[23] C. W. Carlson *et al.*, "FAST observations in the downward auroral current region: Energetic upgoing electron beams, parallel potential drops, and ion heating," *Geophys. Res. Lett.*, vol. 25, no. 12, pp. 2017–2020, 1998.

[24] R. E. Ergun *et al.*, "FAST satellite observations of large-amplitude solitary structures," *Geophys. Res. Lett.*, vol. 25, no. 12, pp. 2041–2044, 1998.

[25] G. Marklund, L. Blomberg, C. G. Fälthammar, and P. A. Lindqvist, "On intense diverging electric fields associated with the black aurora," *Geophys. Res. Lett.*, vol. 21, no. 17, pp. 1859–1862, 1994.

[26] S. B. Ganguli and P. J. Palmadesso, "Plasma transport in the auroral return current region," *J. Geophys. Res.*, vol. 92, no. A8, pp. 8673–8690, 1987.

[27] N. Singh, H. Thiemann, and R. W. Schunk, "Simulations of auroral plasma processes: Electric fields, waves and particles," *Planet. Space Sci.*, vol. 35, no. 3, pp. 353–395, 1987.

[28] R. M. Winglee *et al.*, "Particle acceleration and wave emissions associated with the formation of auroral cavities and enhancements," *J. Geophys. Res.*, vol. 93, no. A12, pp. 14567–14590, 1988.

[29] J. R. Jasperse, "Ion heating, electron acceleration, and the self-consistent parallel E field in downward auroral current regions," *Geophys. Res. Lett.*, vol. 25, no. 18, pp. 3485–3488, 1998.

[30] J. R. Jasperse and N. J. Grossbard, "Ion heating, electron acceleration, and the self-consistent parallel E field in downward auroral current regions," in *Physics of Space Plasmas*, T. Chang and J. R. Jasperse, Eds., 1998, pp. 181–186.

[31] Y. T. Chiu and J. M. Cornwall, "Electrostatic model of a quiet auroral arc," *J. Geophys. Res.*, vol. 85, no. A2, pp. 543–556, 1980.

[32] W. Lennartsson, "Some aspects of double layer formation in a plasma constrained by a magnetic mirror," *Laser Particle Beams*, vol. 5, pp. 315–324, 1987.

[33] J. Lemaire, A. Baraket, J. M. Lescaux, and B. Shizgal, "A method for solving Poisson's equation in geophysical and astrophysical plasmas," *Rarefield Gas Dynam.*, vol. 28, pp. 417–423, 1991.

[34] A. R. Barakat and R. W. Schunk, "Transport equations for multicomponent anisotropic space plasmas: A review," *Plasma Physics*, vol. 24, no. 4, pp. 389–418, 1982.

[35] S. B. Ganguli and P. J. Palmadesso, "Plasma transport in the auroral return current region," *J. Geophys. Res.*, vol. 92, no. A8, pp. 8673–8690, 1987.

[36] T. I. Gombosi and C. E. Rasmussen, "Transport of gyration-dominated space plasmas of thermal origin. I. Generalized transport equations," *J. Geophys. Res.*, vol. 96, no. A5, pp. 7759–7778, 1991.

[37] S. B. Ganguli, H. G. Mitchell, and P. J. Palmadesso, "Behavior of ionized plasma in the high latitude topside ionosphere: The polar wind," *Planet. Space Sci.*, vol. 35, no. 6, pp. 703–713, 1987.

[38] E. Möbius, F. M. Ipavick, M. Scholar, G. Gloeckler, D. Hovestadt, and B. Klecker, "Observations of a nonthermal ion layer at the plasma sheet boundary during substorm recovery," *J. Geophys. Res.*, vol. 85, no. A10, pp. 5143–5148, 1980.

[39] R. Z. Sagdeev and A. A. Galeev, *Nonlinear Plasma Theory*. New York: W. A. Benjamin, 1969, ch. 2.

[40] S. Ichimaru, *Basic Principles of Plasma Physics*. New York: W. A. Benjamin, 1973, ch. 10.

[41] T. Chang, G. B. Crew, N. Hershkowitz, J. R. Jasperse, J. M. Retterer, and J. D. Winningham, "Transverse acceleration of oxygen ions by electromagnetic ion cyclotron resonance with broad band left-hand polarized waves," *Geophys. Res. Lett.*, vol. 13, no. 7, pp. 636–639, 1986.

[42] R. W. Schunk and A. F. Nagy, "Ionospheres of the terrestrial planets," *Rev. Geophys. Space Phys.*, vol. 18, no. 4, pp. 813–852, 1980.

[43] G. Bader and P. Deuflhard, "A semi-implicit mid-point rule for stiff systems of ordinary differential equations," *Numerische Mathematik*, vol. 41, pp. 373–398, 1983.

[44] M. Andre *et al.*, "Ion energization mechanisms at 1700 kilometers in the auroral region," *J. Geophys. Res.*, vol. 103, pp. 4199–4222, 1998.

John R. Jasperse was educated at Harvard University, Cambridge, MA and Northeastern University, Boston, MA, where he received the Ph.D. in physics in 1967.

From 1968 to 1970, he was a Lecturer in the Physics Department at Northeastern University where he taught electromagnetic theory and plasma physics. In 1965, he joined the Air Force Research Laboratory (formerly called the Air Force Cambridge Research Laboratory) located at Hanscom AFB, MA, where he is currently a Group Leader in the Space Physics Models Branch. He has served as a Visiting Scientist at the Massachusetts Institute of Technology Center for Space Research since 1979. His current research interests are in the area of ionospheric and magnetospheric physics and plasma physics.

Dr. Jasperse has received a number of awards, honors, and achievements, including the Marcus O'Day and Guenter Loeser Awards. He is listed in American Men of Science and is a co-convener of the Cambridge Workshop Series in Theoretical Geoplasma Physics. Since 1964, he has authored 87 journal articles, 12 book chapters and conference proceedings, has given numerous lectures at major institutions, and has been a requested consultant for several Department of Defense agencies.

Neil J. Grossbard (M'76) received the B.S. degree in physics from the Massachusetts Institute of Technology in 1959 and the M.S. degrees from Northeastern University in physics in 1962, mathematics in 1971, and electrical engineering in 1981.

He is a Senior Research Physicist at Boston College. His expertise in numerical analysis and modeling methods has enabled him to solve numerous problems in the fields of signal processing and differential, partial differential, and integral equations. Mr. Grossbard has many scientific publications in *Physical Review*, *Journal of Applied Physics*, *Geophysical Research Letters* and other journals.